



NRL/MR/6750--12-9413

Magnetic Field and Geometry Effects on Finding Plasma Potential with a Cylindrical Impedance Probe

D.N. WALKER

*Sotera Defense Solutions, Inc.
Crofton, Maryland*

R.F. FERNSLER

D.D. BLACKWELL

W.E. AMATUCCI

*Charged Particle Physics Branch
Plasma Physics Division*

July 2, 2012

REPORT DOCUMENTATION PAGE				Form Approved OMB No. 0704-0188	
Public reporting burden for this collection of information is estimated to average 1 hour per response, including the time for reviewing instructions, searching existing data sources, gathering and maintaining the data needed, and completing and reviewing this collection of information. Send comments regarding this burden estimate or any other aspect of this collection of information, including suggestions for reducing this burden to Department of Defense, Washington Headquarters Services, Directorate for Information Operations and Reports (0704-0188), 1215 Jefferson Davis Highway, Suite 1204, Arlington, VA 22202-4302. Respondents should be aware that notwithstanding any other provision of law, no person shall be subject to any penalty for failing to comply with a collection of information if it does not display a currently valid OMB control number. PLEASE DO NOT RETURN YOUR FORM TO THE ABOVE ADDRESS.					
1. REPORT DATE (DD-MM-YYYY) 02-07-2012		2. REPORT TYPE Memorandum Report		3. DATES COVERED (From - To)	
4. TITLE AND SUBTITLE Magnetic Field and Geometry Effects on Finding Plasma Potential with a Cylindrical Impedance Probe				5a. CONTRACT NUMBER	
				5b. GRANT NUMBER	
				5c. PROGRAM ELEMENT NUMBER	
6. AUTHOR(S) D.N. Walker,* R.F. Fernsler, D.D. Blackwell, and W.E. Amatucci				5d. PROJECT NUMBER 67-9872-02	
				5e. TASK NUMBER	
				5f. WORK UNIT NUMBER	
7. PERFORMING ORGANIZATION NAME(S) AND ADDRESS(ES) Naval Research Laboratory 4555 Overlook Avenue, SW Washington, DC 20375-5320				8. PERFORMING ORGANIZATION REPORT NUMBER NRL/MR/6750--12-9413	
9. SPONSORING / MONITORING AGENCY NAME(S) AND ADDRESS(ES) Office of Naval Research One Liberty Center 875 North Randolph Street, Suite 1425 Arlington, VA 22203-1995				10. SPONSOR / MONITOR'S ACRONYM(S) ONR	
				11. SPONSOR / MONITOR'S REPORT NUMBER(S)	
12. DISTRIBUTION / AVAILABILITY STATEMENT Approved for public release; distribution is unlimited.					
13. SUPPLEMENTARY NOTES *Sotera Defense Solutions, Inc., Crofton, MD					
14. ABSTRACT A recent rf technique for determining plasma potential, ϕ_p , using an impedance probe is predicted to be independent of probe geometry, magnetic field, and orientation. We test this for a cylindrical probe used in recent studies aimed at finding both ϕ_p and the electron distribution function, $f(\epsilon)$, in the absence of a magnetic field. In the presence of a magnetic field, electron plasma resonances seen by impedance probes are shifted to the upper hybrid frequency, ω_{uh} , and measurements of n_e using a probe of cylindrical geometry can be strongly affected by orientation. However, in this note we demonstrate that measurement of ϕ_p is not. The technique is based on combined experimental and theoretical methods developed in the Charged Particle Physics Branch at the Naval Research Laboratory. Earlier references to our work describe determination of electron density, n_e , and the construction of $f(\epsilon)$ for the cylindrical impedance probe in the absence of a magnetic field. The method has general application to diverse areas of plasma investigations in the laboratory or in space plasma measurement application.					
15. SUBJECT TERMS Plasma sheath Plasma impedance Collisionless plasma Plasma potential					
16. SECURITY CLASSIFICATION OF:			17. LIMITATION OF ABSTRACT Unclassified Unlimited	18. NUMBER OF PAGES 18	19a. NAME OF RESPONSIBLE PERSON William E. Amatucci
a. REPORT Unclassified Unlimited	b. ABSTRACT Unclassified Unlimited	c. THIS PAGE Unclassified Unlimited			19b. TELEPHONE NUMBER (include area code) (202) 404-1022

TABLE OF CONTENTS

<i>I</i>	<i>Introduction.....</i>	<i>1</i>
<i>II</i>	<i>Theoretical Basis for determining ϕ_p.....</i>	<i>1</i>
<i>III</i>	<i>Outline of Experimental Procedure.....</i>	<i>3</i>
<i>IV</i>	<i>Results and Discussion.....</i>	<i>3</i>
	<i>IV.1 Effect of B on impedance probe resonance.....</i>	<i>4</i>
	<i>IV.2 Effect of B on cylindrical Langmuir probes.....</i>	<i>4</i>
	<i>IV.3 $Re(Z_{ac})$ vs V_{bias} at fixed frequencies.....</i>	<i>5</i>
<i>V</i>	<i>Summary.....</i>	<i>6</i>
<i>VI</i>	<i>Figure Captions.....</i>	<i>7</i>
<i>VII</i>	<i>Appendix.....</i>	<i>8</i>
<i>VIII.</i>	<i>References.....</i>	<i>10</i>
<i>IX.</i>	<i>Figures.....</i>	<i>11</i>

I. Introduction

We recently used a small cylinder with a high aspect ratio ($L/r \sim 100$)¹ as an impedance probe in demonstrating the usefulness of network analyzers in plasma diagnostics in the absence of a magnetic field. In that work we determined electron density and temperature (n_e , T_e), plasma potential, ϕ_p , and, the electron energy distribution, $f(\epsilon)$, using the same impedance probe techniques developed for spherical geometry and presented in studies using probes of varying sizes.²⁻⁵ It is well known that n_e , T_e determined using Langmuir techniques to analyze the IV characteristic of a cylindrical probe can be affected by the presence of a magnetic field. Magnetic field effects are a function of probe geometry, bulk plasma parameters and, the magnitude of the field itself. With an impedance probe, electron plasma resonances are shifted to the upper hybrid frequency, ω_{uh} , and measurements of n_e using a probe of cylindrical geometry can be strongly affected by orientation with respect to B . However, measurement of ϕ_p is not. We present three-dimensional surface plots from which ϕ_p may be estimated for varying magnetic fields and probe angle with respect to the field. As in earlier notes, we will not repeat the theoretical framework but will present the equations used in the analysis with only a very brief description. Large parts of the short theoretical basis which appears in **Section II** and the experimental procedure described in **Section III** are taken from earlier work.¹ In addition **Section IV.2** has been included for the sake of completeness in examining magnetic field effects on both impedance probes and Langmuir probes. An Appendix is included to provide the theoretical basis of the restriction on applied frequency in determining ϕ_p as well as considerations related to limits on electron density using the current arrangement. Those interested in the basis of cylindrical Langmuir probe theory in a magnetic field as well as plasma theory related to impedance probes presented in this Note are referred to earlier, more complete, treatments.^{6,7,10,11}

II. Theoretical Basis for determining ϕ_p

The experimental method using a network analyzer is based on determining the real and imaginary parts of the ac plasma impedance from the reflection coefficient². The determination of plasma potential⁴, ϕ_p , along with the electron distribution function, $f(\epsilon)$ ^{4,5} and electron temperature, T_e ³, requires that we operate in the frequency range $\omega_{pi} < \omega < \omega_{pe}(r_0)$, where ω_{pi} is the ion plasma frequency, ω is the applied network analyzer frequency, and $\omega_{pe}(r_0)$ is the electron plasma frequency at the surface of the probe with radius r_0 . The lower bound eliminates an ion contribution since the ions cannot respond at the higher frequency. Also, electron resonant absorption² is removed as a possibility since this occurs at a position where ω is equal to the plasma frequency at that location. Since the smallest value of $\omega_{pe}(r)$ in the sheath region occurs for $r = r_0$, or at the surface of the negatively biased probe, we require that ω be smaller than $\omega_{pe}(r_0)$ to construct the distribution function over as wide a range as possible. The upper bound on energy is ultimately determined by the dc bias voltage at which $\omega_{pe}(r_0) = \omega_{pi}$. In determining ϕ_p however, this restriction is relaxed since at plasma potential there is no sheath and the

aaaaaaaaaaaaaaaa
Ocpwuekr vcr r tqxgf "Cr tkl34."42340'

plasma surrounding the probe is effectively simply the bulk plasma itself. Hence in the region near this potential (but removed from floating potential) it is sufficient to use a frequency $\omega \sim 0.1 \omega_{pe}$ where ω_{pe} bulk plasma frequency. (See the Appendix to this work for an estimate of $\omega_{pe}(r_0)$.) Because of this frequency range, the ac ion current is small and the ac resistance is given by³,

$$R_{ac} = \left(\frac{dI_e}{dV_p} \right)^{-1} \quad (1)$$

where I_e is the dc electron current at bias voltage V_p *i.e.*, the total ac current is now largely electron current. The Druyvesteyn⁹ equation may then be expressed in terms of a first order derivative or,

$$f(\varepsilon) = \frac{4}{e^3 A_p} \sqrt{\frac{m_e \varepsilon}{2}} \left(\frac{dR_{ac}^{-1}}{dV_p} \right)_{eV_p = -\varepsilon} \quad (2)$$

and thus noise is reduced in the calculation of the distribution function, where A_p is the probe area, m_e is electron mass, and ε is the energy. We note that in this expression there is no geometry dependence. In addition, our earlier work³ demonstrates the relationship between the real part of the analyzer output and R_{ac} ,

$$\text{Re}(Z_{ac}) = \frac{R_{ac}}{1 + (\omega R_{ac} C_{ac})^2}. \quad (3)$$

Therefore, in the frequency range given, and provided $\omega R_{ac} C_{ac} \ll 1$, we have $\text{Re}(Z_{ac}) \approx R_{ac}$ and $\text{Re}(Z_{ac})$ from the network analyzer output can be directly used in place of R_{ac} in Eqn (2). This simplifies finding $f(\varepsilon)$ by avoiding a calculation for R_{ac} when reducing the data.

Since the basis for determining plasma potential is that $d^2 I_e / dV_p^2$ vanishes at $V_p = \phi_p$,

$$\left. \frac{dR_{ac}}{dV_p} \right|_{V_p = \phi_p} = -R_{ac}^2 \left(\frac{d^2 I_e}{dV_p^2} \right) \bigg|_{V_p = \phi_p} = 0 \quad (4)$$

and finally,

$$\left. \frac{d \text{Re}(Z_{ac})}{dV_p} \right|_{V_p = \phi_p} \approx 0 \quad (5)$$

Plots of the network analyzer output of $\text{Re}(Z_{ac})$ versus applied bias for frequencies in the range specified will then show a minimum at $V_p = \phi_p$. (Due to the dependence of $f(\varepsilon)$ on dR_{ac}^{-1}/dV_p seen in Eq (2) we are able to construct $f(\varepsilon)$ in the vicinity of ϕ_p for small negative bias voltages and from this derive n_e and T_e as covered in earlier work cited above.)

III. Outline of Experimental Procedure

We refer the reader interested in the experimental details to the earlier works and only provide an outline of that same description here.

The experiments were conducted using as a probe a stainless steel cylinder with length, $L = 15$ cm and radius, $r = 0.16$ cm which is connected to an HP8735D Network Analyzer through 50 Ω coaxial cable which provides the driving signal. This arrangement including the chamber, analyzer and the coupling circuitry is shown schematically in Reference 2. The cylinder is mounted on a 1/4 inch diameter ceramic and steel support which is connected to 1/4 inch diameter semi-rigid copper 50 Ohm coaxial cable.

The determination of plasma impedance depends upon the network analyzer measurement of the complex reflection coefficient, $\Gamma(\omega)$. The analyzer returns as separate outputs $Re Z_{ac}(\omega)$ and $Im Z_{ac}(\omega)$ where,

$$Z_{ac}(\omega) = Z_0 \left[\frac{1 + \Gamma(\omega)}{1 - \Gamma(\omega)} \right] \quad (6)$$

and $Z_0 (=50 \Omega)$ is the internal impedance of the analyzer. We also note that the ratio of reflected-to-total power is given by,

$$|\Gamma|^2 = \frac{P_r}{P_0} \quad (7)$$

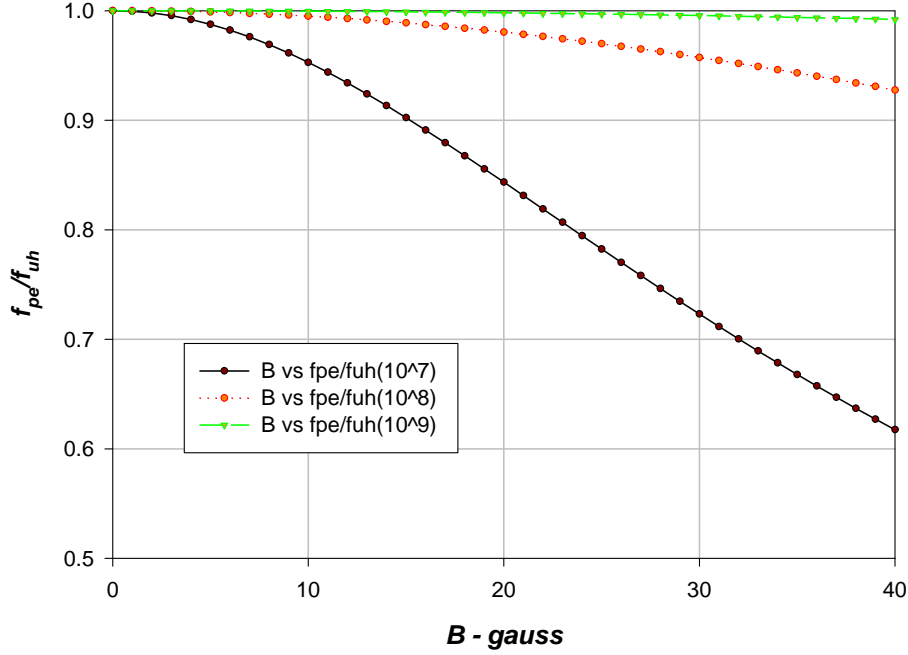
where $P_0 = P_R + P_T$ with P_R and P_T the reflected and transmitted powers, respectively. (The quantity $1 - |\Gamma|^2$ is the normalized transmitted power and this output is also available).

IV. Results and Discussion

We examine a data set comprised of values of $Re(Z_{ac})$ for varying angle of the probe from 0 to $\pi/2$ with respect to B . In addition, the magnetic field covered the range 2-40 gauss and most data sets were taken using a set network analyzer frequency of 10 MHz. For these data $f_{pi} \approx 3 \times 10^5$ Hz and $f_{pe}(\text{bulk plasma}) \approx 200$ MHz. We provide also two separate independent determinations of ϕ_p for comparison using: (1) an independent (small) Langmuir probe in addition to, (2) the (large) impedance probe itself swept as a Langmuir probe.

IV.1 Effect of B on impedance probe resonance

For those cases in which the electron plasma frequency, f_{pe} , is comparable to the electron cyclotron frequency, f_{ce} , the impedance probe resonance will occur at the upper hybrid frequency, f_{uh} . For comparison to our general plasma parameter regime we provide a plot of the ratio of f_{pe} to f_{uh} . Each trace corresponds to a different plasma density. As indicated in the legend the density varies from 10^7 to 10^9 cm^{-3} . Since the density range 10^8 - 10^9 cm^{-3} is most representative of the work here, we expect little effect on the determination of density from the primary resonance except at the highest field.



IV.2 Effect of B on cylindrical Langmuir probes

With a cylindrical probe aligned along B , magnetic field effects under certain restrictions can decrease the collected electron current and therefore Langmuir probe determination of density based on electron saturation current collection indicates an artificially lower bulk plasma value than is the actual case. Because of this, electron

temperature determinations can also be compromised since most fitting routines use the entire IV characteristic in the fit itself. The effects of magnetic fields on both spheres and cylinders have been studied over the years^{6,7}, and it is not the intention here to retrace that work although some general comments are appropriate when comparing to impedance probe measurements. The magnitude of the effect depends on the electron gyroradius, r_e , in addition to the size and shape of the probe and its sheath. In a thin sheath limit, and assuming the same applied bias, we expect generally less influence as a function of probe orientation with respect to \mathbf{B} as probe radius, r , decreases with respect to r_e . In the present case the sheath radius, r_{sh} is estimated at 0.5 cm (assuming $r_{sh} \sim 5\lambda_D$) while the cylinder radius is 0.16 cm or $r_{sh} > r$. Also, since r_e/r for a 2 gauss confining field is of order 10 for a typical T_e of 1 eV, we expect less of an effect than would be the case for a lower ratio. However, it has been shown for cylindrical probes that even when $r_e > r$ magnetic fields can be important and, in addition, even extending to the case where r_{sh} is comparable to r_e .⁸ To avoid complications associated with inferring density from the electron saturation current when operating in a magnetic field using conventional analysis techniques, ion saturation current is often used instead where,

$$I_{ion} = A_p e n_0 \sqrt{\frac{T_e}{m_e}} e^{-0.5} \quad (8)$$

The factor $e^{-0.5} = e^{-e\phi/T_e}$ arises from the density decrease at the sheath edge (where quasineutrality applies at the bulk plasma) to the pre-sheath. With the ion flow velocity at the sheath edge taken as the ion sound speed, ion energy and flux conservation require approximately that $e\phi(r_{sh}) = T_e/2$ and the Boltzmann condition then allows,

$$n_{ion}(r_{sh}) = n_0 e^{\frac{-e\phi(r_{sh})}{T_e}} = n_0 e^{-0.5} \quad (9)$$

Since the ion gyroradius is typically much larger than probe dimensions, and if the sheath is small, there is no effect on I_{ion} from a large range of magnetic field magnitudes. *i.e.*, the ions are unmagnetized. The value determined however may still be compromised by the structure of the fitting routine used to analyze the characteristic *i.e.*, density determined from even the ion saturation level can be incorrect since the data reduction technique typically applies a fit to the entire IV characteristic, a portion of which is the electron saturation current region. Also, the existence of a high energy electron component added to the bulk population can complicate this analysis⁸ but for a MB distribution the analysis is justified.

IV.3 $Re(Z_{ac})$ vs V_{bias} at fixed frequencies

We plot in Figures 1 and 2 different views of $Re(Z_{ac})$ vs V_{bias} at fixed frequencies. The plots from which plasma potential is obtained as described in the earlier works cited are shown in Figure 1. Also, these are the primary plots from which the values of $Re(Z_{ac})$ are derived for use in the construction of $f(\epsilon)$. Figure 2 is presented as 3D contours to

show in one figure the dependence of the minimum on both the magnitude of B and the angle of the probe with respect to B . The contour levels are chosen to be fairly wide to indicate the general level of ϕ_p in a different view and to make the contours showing dependences on B and the angle smoother. The values themselves are more easily determined in the plots of Figure 1. The local minima at roughly 2 volts in these figures are consistent with the determination of V_p from a Langmuir probe-based characteristic analysis with the exception of the field-aligned probe for B greater than 10 gauss. (For increasing B , current collected by the probe when field-aligned is, in the absence of collisions, reduced considerably because of the reduced cross-section. At some point this current becomes negligible and therefore determination of R_{ac} undefined. In plots shown in Figure 1 this begins at 20 gauss or at $r_{Le} \sim 0.1$ cm and continues into the higher field region plots.) In addition, Figures 3 and 4 show plasma potential as measured by sweeping both the impedance probe (Figure 3) and a small Langmuir probe during the angular variation period (Figure 4) at differing fields. The latter measurement was taken for an independent comparison mainly to determine whether the variations measured in ϕ_p are due to angular and field magnitude variations, or a characteristic variation of the plasma over the time interval necessary to perform the measurements on the primary (large) probe being studied. Since these variations appear to closely follow both impedance probe determinations of ϕ_p , along with Langmuir sweeps of the same probe using a conventional algorithm which searches for a peak in the 2nd derivative, we are inclined to conclude that the variations seen are actual plasma frequency variations which may be influenced by the field but do not appear to be a function of the probe angle with respect to the field. Our conclusion from these observations is that for the electron density and temperatures selected, the determination of ϕ_p is not influenced by the probe geometry, the magnitude of B or the angle with respect to the field.

V. Summary

Over the past three years using spheres of different sizes as rf impedance probes, we have developed a technique which includes determining plasma potential and the electron distribution function. The theoretical basis for this work found in the references suggests that the technique is, to a large degree, independent of probe geometry. The work presented here, using a cylindrical probe with a high-aspect ratio, is consistent with this conclusion.

VI. Figure Captions

Figure 1 – 2D plots of the $Re(Z_{ac})$ for varying angles with respect to magnetic field, B , and different probe bias levels. Each plot is for a different B varying from 2 gauss to 40 gauss. The plots may be compared to Figure 2 below. As the angle decreases at the higher field strengths, it can be seen that the minimum in $Re(Z_{ac})$ is less well-defined and is not seen at all at the position of greatest field alignment ($\theta = 0$). This particular feature is not easily discernible in the 3D surface plots of Figure 2.

Figure 2 – 3D-Surface plots of the $Re(Z_{ac})$ for varying angles with respect to magnetic field, B , and different probe bias levels. Each plot is for a different B varying from 2 gauss to 40 gauss. The plots have been structured to give broad areas showing minima as predicted by theory.

Figure 3 – A plot of plasma potential, ϕ_p , as measured by a small Langmuir probe in the approximate area of the large probe during variation of the orientation of the large probe with respect to B .

Figure 4 – A plot of plasma potential, ϕ_p , as measured by the large impedance probe when used as a Langmuir probe during variation of the orientation with respect to B .

Figure 5 – A plot of $Re(Z_{ac})$ vs probe bias for varying densities. Included also is a plot of plasma potential as determined by conventional Langmuir probe sweep analysis of the same probe. The run number given as the abscissa of the plot of plasma potential corresponds to one of the five densities beginning with the highest ($4.5 \times 10^7 \text{ cm}^{-3}$) and proceeding to the lowest ($7 \times 10^5 \text{ cm}^{-3}$)

VII. Appendix

On an estimate of $\omega_{pe}(r_0)^{10,11}$

Although the determination of plasma potential is not subject to such stringent conditions on the upper frequency bound as mentioned above, it is useful to provide an estimate of density at the probe surface when determining the possibility of constructing $f(\epsilon)$ for parameter regimes including densities of 10^8 cm^{-3} and lower. Often the requirement for low density plasmas and low temperature electrons can severely limit the usefulness of this technique in determining $f(\epsilon)$ because of noise problems associated with interpreting network analyzer results at low frequencies. The estimates in this section apply for a planar and not a spherical probe. The results however remain valid in the thin sheath limit

We assume collisionless plasma and that the ion flux into the plasma sheath is given by,

$$\phi = n_s v_B = n_s \sqrt{\frac{kT_e}{M}} \quad \text{A.1}$$

where v_B is the Bohm speed, M is ion mass, and n_s is ion density at the sheath edge. In shortened form,

$$\phi = n_s 9.79 \times 10^5 \left(\frac{T_e}{\mu}\right)^{\frac{1}{2}} \quad \text{A.2}$$

with T_e in eV and μ is ion mass in amu. The electron speed at the probe is,

$$v_e = \sqrt{\frac{T_e}{2\pi m_e}} = 4.19 \times 10^7 \sqrt{\frac{T_e}{2\pi}} \quad \text{A.3}$$

From the Boltzmann relation, the density at the probe is,

$$n(r_0) = n_s e^{\frac{-V_s}{T_e}} \quad \text{A.4}$$

where V_s is the voltage drop from the probe surface to the sheath edge and r_0 is the probe radius assuming a spherical probe. When the probe is at floating potential, ion and electron currents are equal by definition and we find,

$$V_s = \left(\frac{1}{2}\right) T_e \ln\left(\frac{M}{2\pi m_e}\right) \quad \text{A.5}$$

(We point out here that the actual equation of V_s for a spherical probe includes a geometric factor $-2T_e \ln(r_s/r_0)$ with $r_s > r_0$ being the sheath radius. This factor which is small compared to the lead term in Eqn (A.5) arises because the total ion flux is given by $n_s v_B (4\pi r_s^2)$ while the electron flux is $n_s v_e (4\pi r_0^2) e^{-V_s/T_e}$.)

For argon ($M=40$ amu) the log factor is ~ 9.38 . Assuming 1 eV electrons we find $V_s/T_e \sim 4.7$ or $n(r_0) \sim .009 n_s$. If the probe is biased more negative from floating potential this estimate of density at the probe would decrease even further. We note that in the present case for a plasma of density $5 \times 10^8 \text{ cm}^{-3}$ as representative, $f_{pe} \sim 200$ MHz. This would imply from above that $f_{pe}(r_0) \sim 1.9$ MHz. For lower T_e , the upper bound on applied frequency is more restrictive. Once again this estimate of the upper limit applies primarily to construction of $f(\varepsilon)$ from the plots of R_{ac} vs V_{bias}

On impedance issues as a function of density

We plot in Figure 5 an illustration of an effect of varying electron density on the determination of φ_p using the method outlined. In this case we continued using a sweep frequency of 10 MHz which for the densities used in the Figures above is appropriate as discussed earlier. However, for the two lower density levels in Figure 5, 10 MHz is too high for the probe geometry based on theoretical estimates. (Note that $f_{pe} \sim 9$ MHz at a density of $n_e = 10^6 \text{ cm}^{-3}$. Since at plasma potential there is no sheath, this would imply from the earlier work² that the applied frequency should be no greater than 2-3 MHz to avoid resonant absorption issues with the bulk plasma. Further considerations on the limit of this frequency versus probe size and electron density will follow in a separate analysis in a future work.) Given the restriction that the frequency should have been lower, it is nevertheless clear from this plot that for the final two densities ($n_e = 2.7 \times 10^6 \text{ cm}^{-3}$ and $7.0 \times 10^5 \text{ cm}^{-3}$), it is not possible to determine a minimum in the noisy traces. The purpose in presenting this in spite of the frequency issue is to illustrate another problem area which arises at lower densities (as in space) and is related to the output impedance of the network analyzer. As the electron density decreases, the dc impedance of the probe to the plasma increases. To the point that high kohm levels of the dc impedance are observed as seen in Figure 5. Since the output impedance of the network analyzer is 50 ohms there is a large mismatch. As a result, the signal-to-noise ratio as a function of applied voltage decreases as well. This suggests that since 50 Ohms is a characteristic impedance of many laboratory instruments including the network analyzer, a circuit which supplies a higher input impedance may be necessary in order to use these analysis techniques in low density plasma. We are currently working toward a solution of this problem.

VIII. References

¹D.N. Walker, R.F. Fernsler, D.D. Blackwell, W.E. Amatucci, *NRL Memorandum Report*, **6750-11-9331** (2011)

²D.N. Walker, R.F. Fernsler, D.D. Blackwell, W.E. Amatucci, and S.J. Messer, *Phys. Plasmas* **13**, 032108 (2006)

³D.N. Walker, R.F. Fernsler, D.D. Blackwell, W.E. Amatucci, *Phys. Plasmas* **15**, 123506 (2008)

⁴D.N. Walker, R.F. Fernsler, D.D. Blackwell, W.E. Amatucci, *Phys. Plasmas* **17**, 113503 (2010)

⁵D.N. Walker, R.F. Fernsler, D.D. Blackwell, W.E. Amatucci, *NRL Memorandum Report*, **6750-10-9237** (2010)

⁶J.G. Laframboise, (PhD Thesis) Univ. of Toronto, *Institute for Aerospace Studies, Report No. 100*, (1966)

⁷J.G. Laframboise and J. Rubinstein, *Phys. Fluids*, **19**, 1900 (1976)

⁸E.P. Szuszcwicz and P.Z. Takacs, *Phys. of Fluids*, **22**(12), 2424 (1979)

⁹M.J. Druyvesteyn, *Physica* **10**, 69, 1930

¹⁰R.F. Fernsler, *Plasma Sources Sci. and Technol*, **18**, 014012 (2009)

¹¹M.A.Lieberman and A.J.Lichtenberg, *Principles of Plasma Discharges and Materials Processing*, 2nd Edition, p. 172, John Wiley and Sons, Inc. NY, 2005

IX. Figures

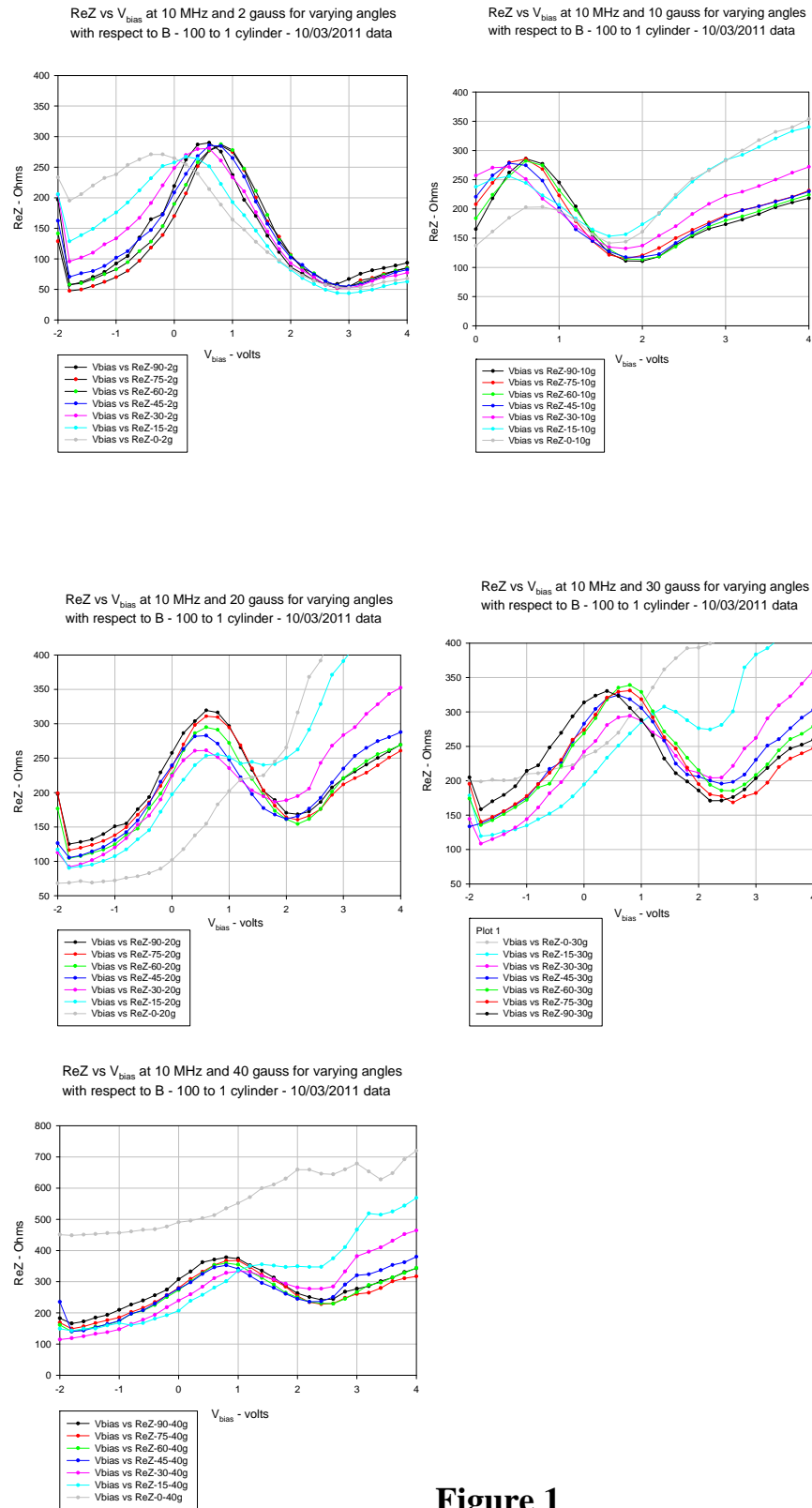


Figure 1

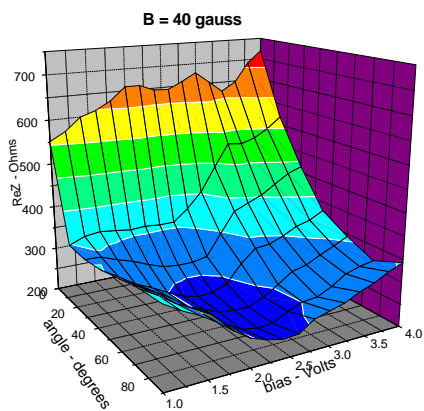
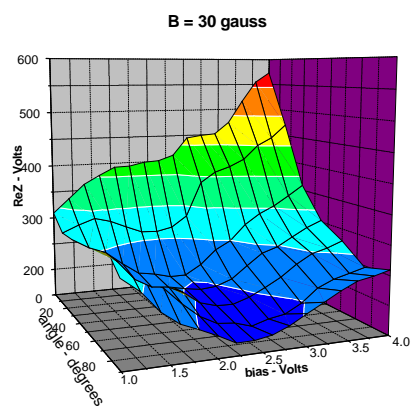
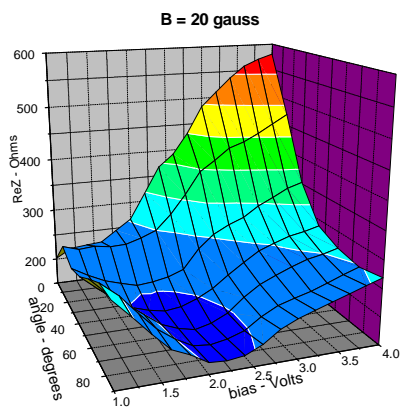
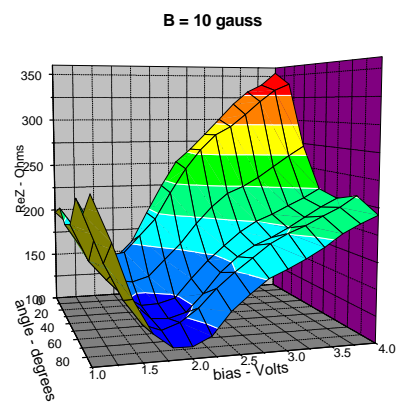
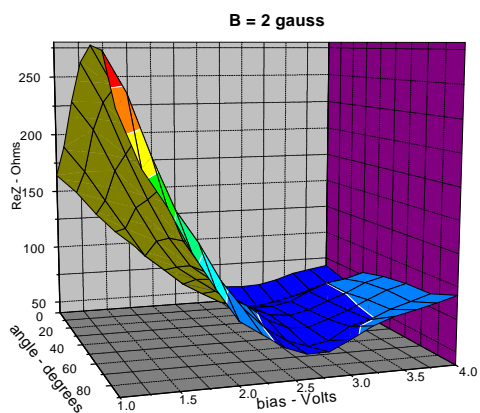


Figure 2

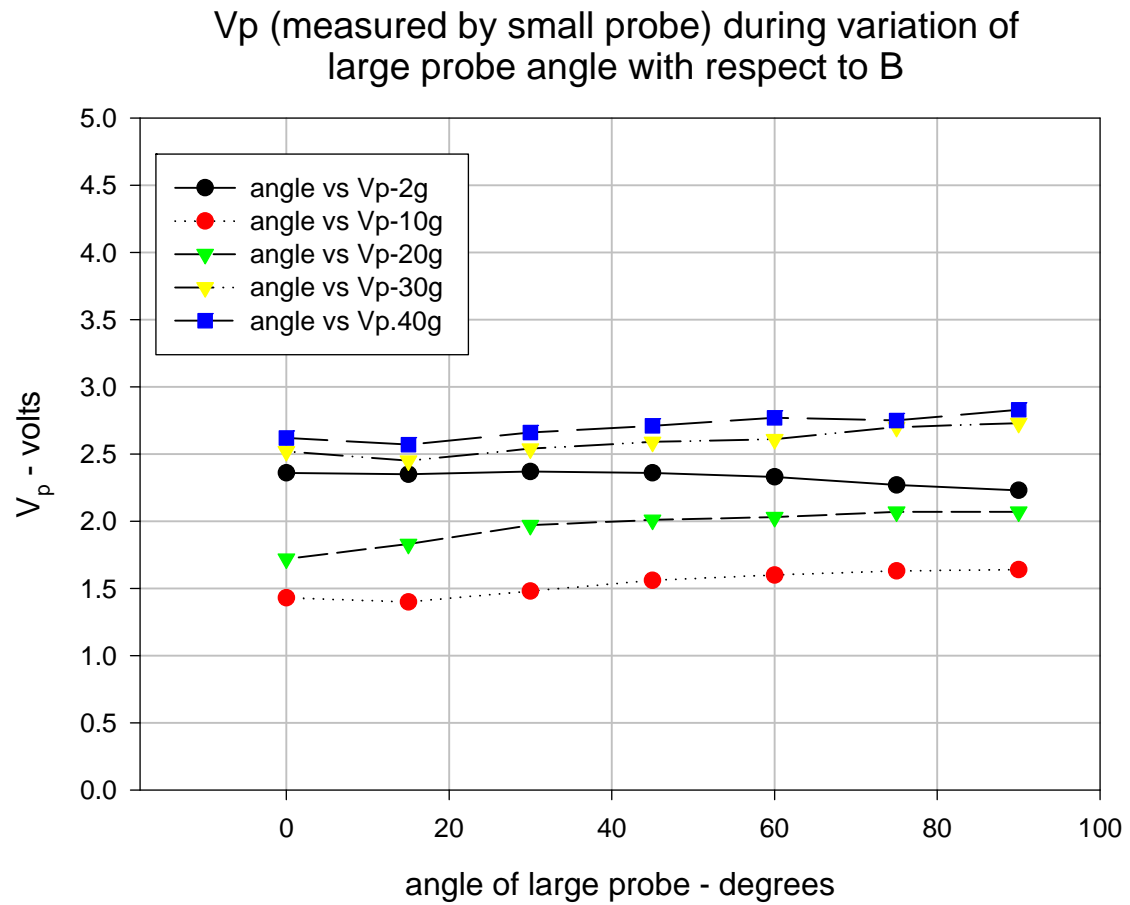


Figure 3

V_p vs angle for varying B - large probe

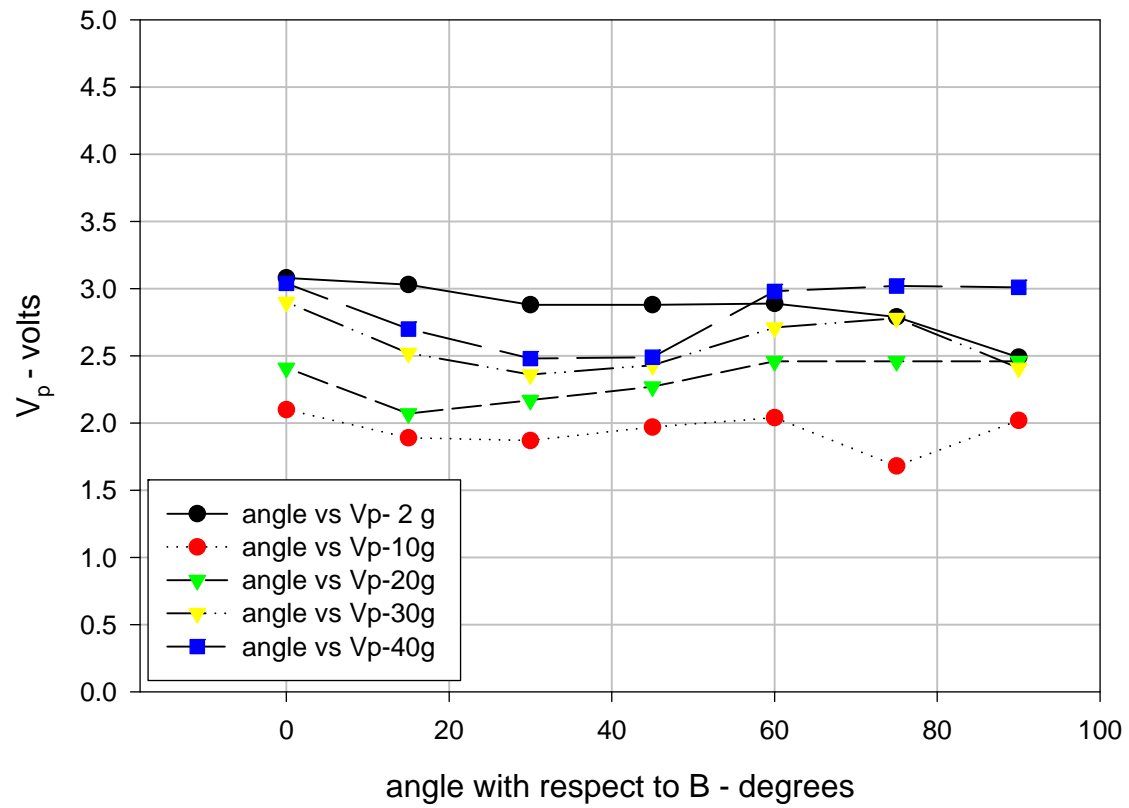


Figure 4

$\text{Re}(Z_{ac})$ vs V_{bias} for varying density - 04042012 data
large cylindrical probe (Area = 15 cm²); B = 0

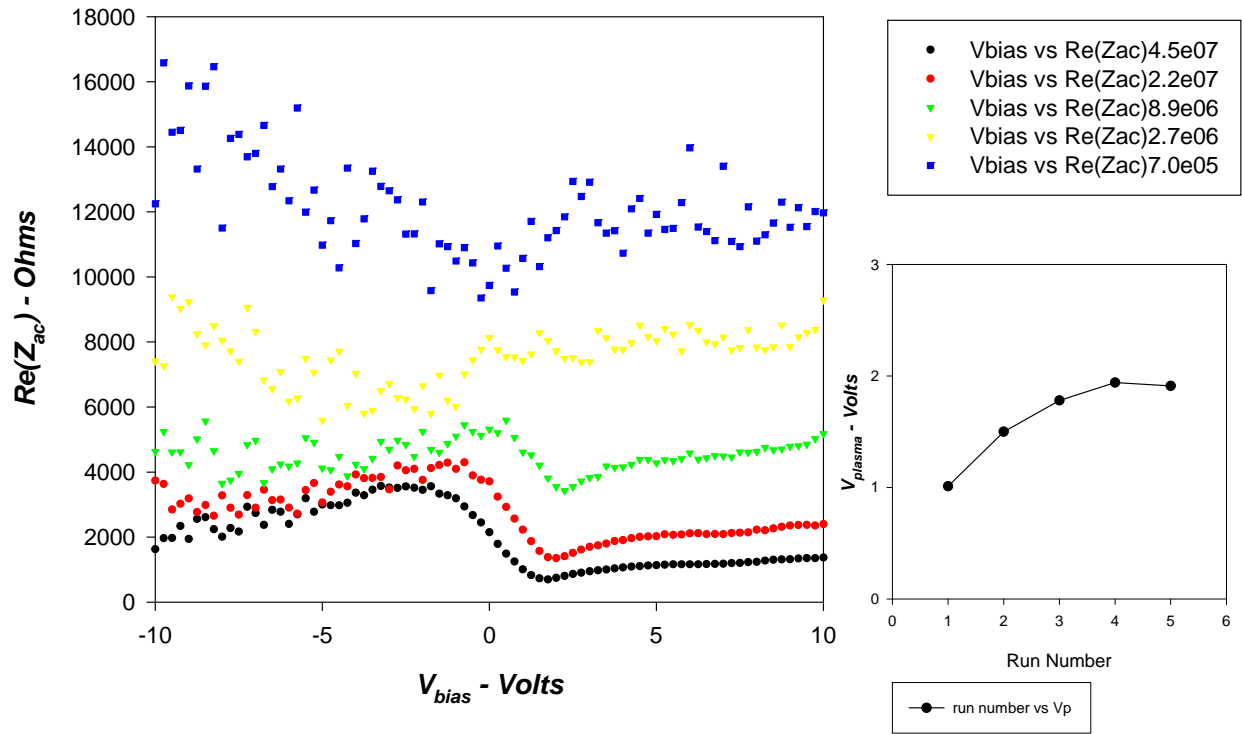


Figure 5